Electrospark method for obtaining nanopowders

M Zhuravlev, R Sazonov, G Kholodnaya, I Pyatkov and D Ponomarev

National Research Tomsk Polytechnic University, 30 Lenin Ave., 634050, Tomsk, Russia

E-mail: galina_holodnaya@mail.ru

Abstract. In the paper, a metallic Fe_xO_y nanopowder was obtained by the electrospark method. The used electrospark installation consists of the electrode system, mobility system, system for measuring processing parameters (oscilloscope and current sensor, HV voltage divider, manovacuum meter), source of current pulses, vacuum system (vacuum pump, gas cylinders with working gas, gas routes, gas taps). The specific feature of the installation is the use of a power supply circuit of two generators with different voltage levels operating for one interelectrode gap. This generator circuit makes it possible to change the treatment parameters in wide ranges (pulse duration 10–100 μs, pulse energy 0.1–0.6 J, pulse repetition rate 0.1–5 kHz). It will enable to choose the optimal ratio between the energy expended and the maximum yield of the product, as well as to study the influence of treatment parameters on the composition and properties of the resulting powder. The morphology and phase composition of the Fe_xO_y synthesized metal powder was studied.

1. Introduction

The development of energy-saving, environmentally friendly methods for obtaining nanopowders of various substances is an important issue of modern science. This is due both to the practical need to create nanomaterials, which ensure their widespread use, and the fundamental need to understand the processes that occur in the production and use of nanoparticles by the methods [1, 2]. High-purity, weakly agglomerated nanopowders are most widely spread. Such nanopowders are used for catalysis, as well as in ecology and medicine [3, 4]. Targeted drug delivery, immobilization of enzymes and drugs, cell hyperthermia, medical diagnostics, wastewater treatment are the main areas of application for magnetic nanomaterials (for example, iron oxide) [5–11]. The large specific surface area of these nanomaterials increases their sorption capacity, and the nanoparticles themselves can be easily captured using a gradient magnetic field [12, 13].

The literature describes various methods for producing iron oxide nanoparticles, including deposition, sol-gel, microemulsion, thermal decomposition, etc. [14–16]. A brief review based on scientific works, including data for the last two decades, is presented in [14]. The paper presents the methods for producing iron oxide nanoparticles, as well as methods for studying their characteristics. The main parameters affecting the structure and size of iron oxide were determined in [17] using the sol-gel method (reaction rate, temperature, nature of the precursor and pH), for example, γ-Fe_2O_3 with a particle size of 6 to 15 nm after heat treatment at 673 K. However, there are some disadvantages of using the sol-gel method: high-energy consumption due to the use of high temperatures in the synthesis process; and the required use of catalysts, which must be removed from the final product at the end of the process.

The microemulsion method is widely used for the synthesis of catalytic iron oxide, because it allows the synthesis of particles with a narrow particle size distribution (from 4 to 15 nm) and a specific surface area (315 $m^2 \cdot g^{-1}$). The disadvantages of this method include the use of expensive surfactants [18].

The method of thermal decomposition of iron-containing precursor (ferric (III) acetylacetonate, iron nitrosophenylhydroxylamine or iron pentacarbonyl) in octyl ether and oleic or lauric acids followed by oxidation, leads to the formation of iron oxide nanoparticles with particle size distribution between 4 and 16 nm. This preparation method produces monodispersed particles with a narrow size distribution, but has a great disadvantage that the resulting particles are always dissolved in non-polar solvents [19]. The purpose of this work is the synthesis of nanosized iron oxide using an electrospark method and the study of their structural features.

2. Experimental setup

The method of the electrospark method for producing metal nanopowders is based on the use of the energy of an electric spark discharge generated between the electrode tool and the sputtered surface. When a voltage pulse is applied between the electrode and the sputtered surface, a plasma channel of a spark breakdown with an initial diameter of RK ~ 0.1 mm is formed. The current flowing through the channel heats it, the pressure in the channel increases, the channel expands. The plasma temperature reaches the values of 3.8×10^4 K, the energy flux density is 10^6–10^9 $J \cdot m^{-2}$. The channel plasma energy transmitted to the surface leads to a rapid (10^{-4}–10^{-7} s) local heating, melting, and evaporation of the metal. As a result of the action of gas-dynamic forces, “metal vapor” is removed from the zone of action of the discharge. Cooling down in the gas of atmospheric pressure, the vapor is condensed on the walls of the glass to collect in the form of nanopowder. The scheme of the experiment is shown in figure 1.

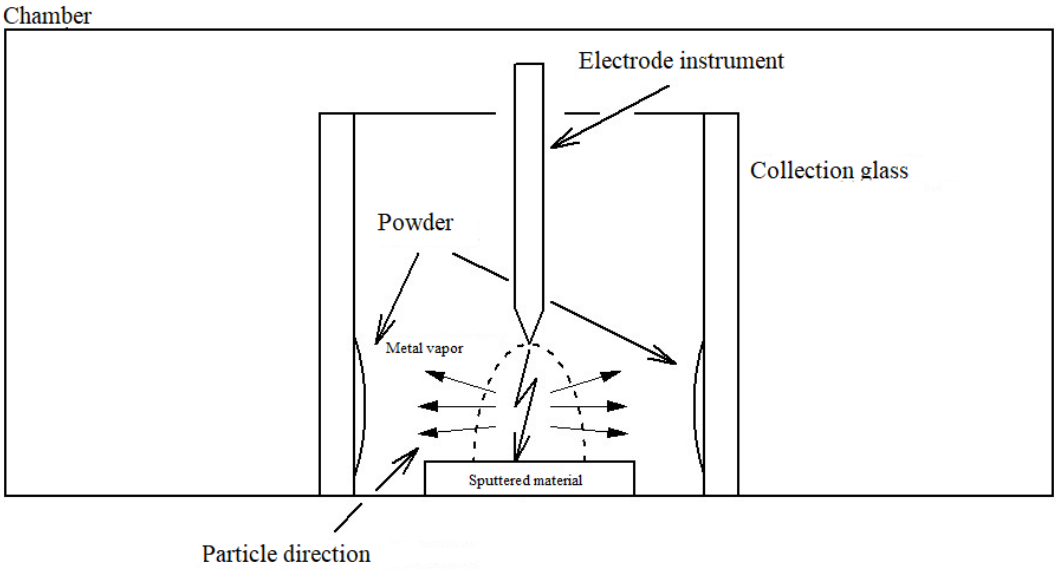

Figure 1. The general scheme of the experiment.

To produce nanopowders, we used two high-voltage generators with current pulse durations of 100 ns and 10 μs. When using a generator with a pulse duration of 10 μs, the productivity of the process of nanopowder formation is 80% higher than when using a generator with a pulse duration of 10 ns. However, with long-term use of the generator with a pulse duration of 10 μs, intense erosion of the tool electrode occurs, which leads to an increase in the interelectrode gap and, as a consequence, a change in the conditions of powder synthesis.

A series of experiments was carried out. The first series of experiments was carried out on the production of two-valence iron (FeO). The samples of cold-rolled steel 08KP were preliminarily

prepared to produce nanopowders. The samples were annealed in a muffle furnace at a temperature of 600°C. As a result, a scale film (FeO) with a thickness of 10–20 μm was formed on the samples, which served as the material for the production of the powder. To prevent the formation of another type of oxide, the powder was produced in a neutral gas – argon. For the synthesis of nanopowder, a generator with a pulse duration of 10 μs was used.

The second series of experiments on the production of iron oxide powder was carried out in an atmosphere of air, the sputtered surface was used as the surface of the samples from cold-rolled steel 08KP in without preliminary treatment. As a result, a red-black nanopowder with pronounced magnetic properties was formed. Samples obtained during the first series of experiments are designated as sample 1, in the second series of experiment – sample 2. For the synthesis of nanopowder, a generator with a pulse duration of 100 ns was used.

The morphology of iron-containing nanooxides was studied by transmission electron microscopy using a JEOL-II-100 electron microscope (Jeol Ltd., Japan). The crystal structure of the Fe_xO_y nanoscale powder was studied using the standard X-ray phase analysis method (Shimadzu XRD-7000S X-ray diffractometer, Shimadzu, Japan).

3. Results and discussion

Figures 2 and 3 present the photos with characteristic images of the morphology of the resulting iron oxide.

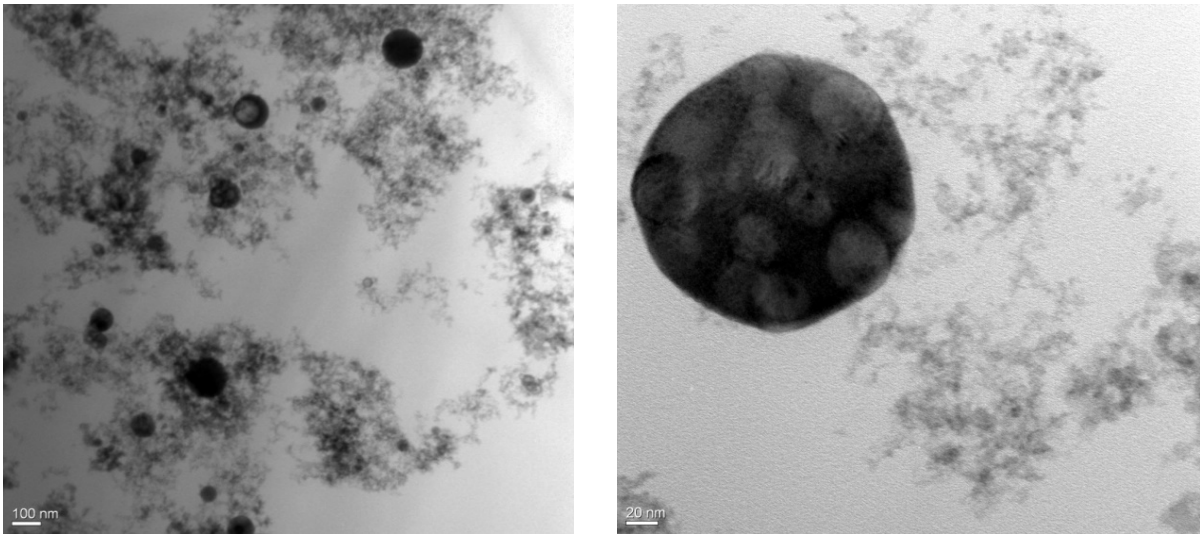

a) b)

Figure 2. TEM images of nanoscale Fe_xO_y obtained in the first series of experiments.

The particles in samples 1 and 2 are mainly clusters in the form of balls with an average size of 5–20 nm. Separate round particles with an average particle diameter of 50–150 nm are observed (figure 2b). In addition, in sample 1 there are individual round hollow particles, the diameter of which does not exceed 100 nm (figure 2a). For sample 2, the morphology of the particles is represented by aggregated particles. It is seen that the particles have a spherical or faceted shape. Smaller particles are combined in clusters, the size of particles in clusters does not exceed 40 nm (figure 3b). Figure 3a shows the formation of a thin layer on the surface of round and large particles. The thickness of the layer did not exceed 4 nm.

In addition to TEM photographs of the synthesized particles, microdiffractograms were taken (figure 4 and 5). For sample 1 on microdiffraction patterns, bright reflections characteristic of the corresponding iron oxide lattices were observed regardless of the particle morphology.

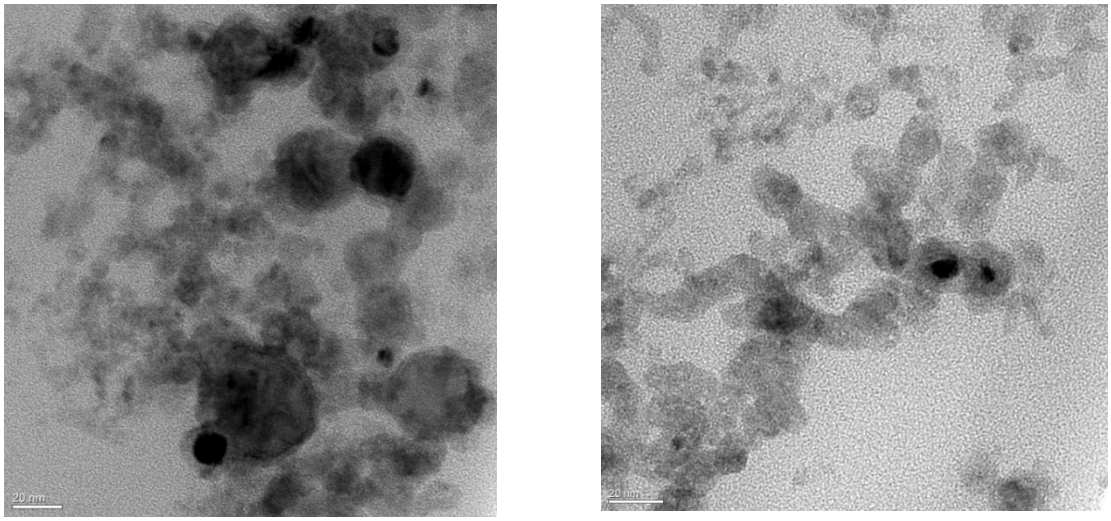

a b

Figure 3. TEM images of nanoscale Fe_xO_y obtained in the second series of experiments.

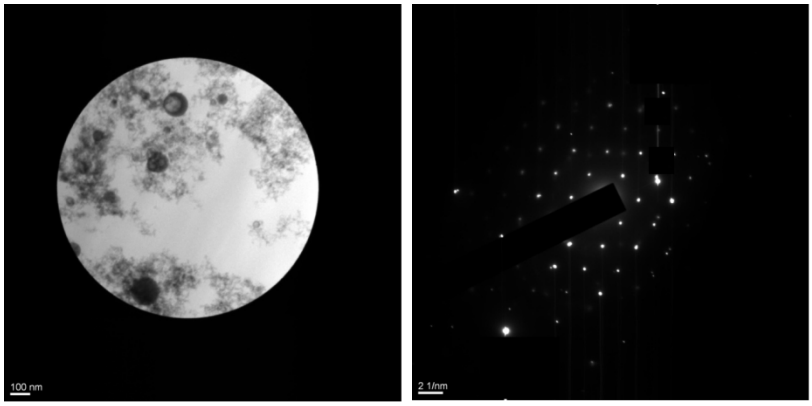

Figure 4. TEM images of Fe_xO_y sample particles and its microdiffraction pattern obtained in the first series of experiments.

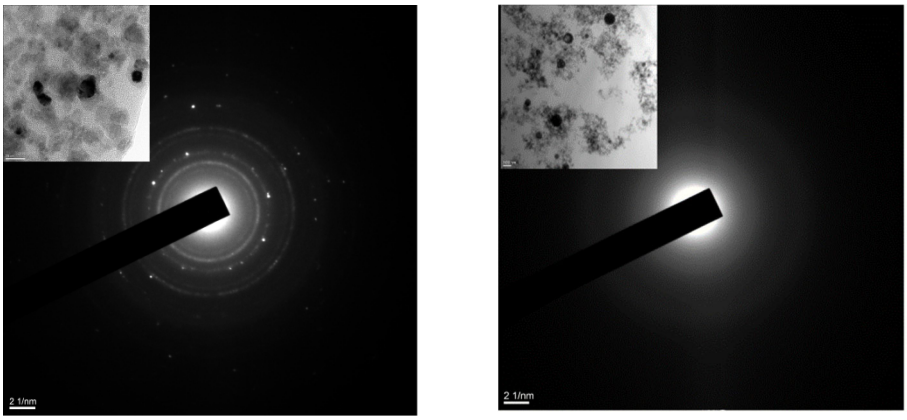

Figure 5. TEM images of Fe_xO_y sample particles and its microdiffraction pattern obtained in the second series of experiments.

For sample 2, it was observed that some particles give bright reflexes on the microdifraction pattern. This is characteristic of particles whose morphology is represented by a faceted form. But for some particles, reflexes were not detected, but a halo was observed, which is responsible for the amorphous state, which is also seen on the radiograph as an X-ray amorphous plateau in the region of small angles.

Figure 6 presents the results of the study of the phase composition of Fe_xO_y nanopowders.

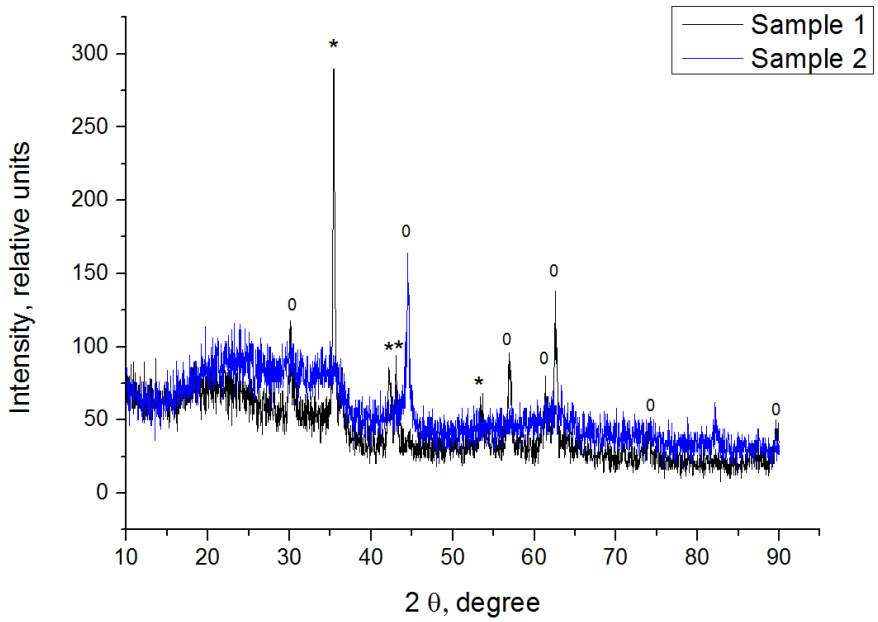

Figure 6. X-ray diffraction patterns of the samples Fe_xO_y (0 – is Fe_2O_3-gamma, * – is FeO-alfa).

X-ray phase analysis showed the presence of the crystal lattice of Fe_2O_3-gamma, FeO-alfa. X-ray phase analysis showed the presence of mostly FeO, which coincides with the composition of the initial oxide film.

For the Fe_xO_y sample obtained in the first series of experiments, an EDS analysis was performed (figure 7).

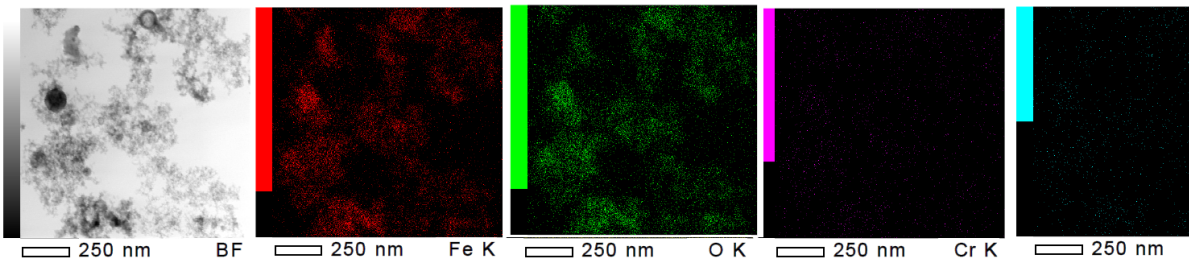

Figure 7. The color windows reflecting the elements of sample 1.

Figure 7 shows that the main elements of iron nanooxide are iron and oxygen. The elemental composition of the powder of sample 1 is represented by Fe – 52%, O – 39%, C – 8%, Cr, Mn, and others – 1%. The carbon content is much higher than in the target material, which is associated with the use of an oily high-pressure vacuum pump for preliminary pumping out of the working chamber. A high percentage of iron indicates the presence in the sample of non-oxidized iron, which is most likely in

amorphous form. The presence of such elements as Cr, Mn can be explained by the fact that these elements are in the target, from which the iron nanooxide was formed.

4. Conclusion

Thus, iron oxide nanopowders were obtained using the electrospark method. Analysis of the powders showed that the pulse duration (10 μs and 100 nm) hardly affects the size of the synthesized nanoparticles. Depending on the medium (argon, air) in which the powders were synthesized, the samples can change color (black, red, red and black), phase composition and oxygen content. The average size of the synthesized particles is in the range of 5–20 nm, there are some larger particles, but not in large quantities, which average size did not exceed 50–150 nm. Particle morphology is represented by both individual circular particles and particles with a faceted shape as well as particles in the form of hollow spheres. The phase composition of the samples is represented by two crystal lattices of Fe_2O_3-gamma, FeO-alfa. The content of the amorphous phase in the second sample is higher. For a sample synthesized in an air atmosphere, encapsulation is observed. The thickness of the shell does not exceed 6 nm. The composition of the shell is probably more oxygenated iron oxide than the core material. The synthesized iron oxides will be used as a core for the further production of a composite in the form of $Fe_xO_y@SiO_2$, Fe_xO_y-TiO_2, etc. (core-shell) for use in catalysis and medicine.

Acknowledgements

This work was supported by Russian Science Foundation (project No. 18-73-10011).

References

[1] Snider G and Ariya P 2010 *Chemical Physics Letters* **491** 23
[2] Peng T, Zhao D, Dai K, Shi W and Hirao K 2005 *Journal of Physical Chemistry B* **109** 4947
[3] Luo X, Morrin A, Killard A J and Smyth M R 2006 *Electroanalysis* **18** 319
[4] Shinkai M 2002 *Journal of Bioscience and Bioengineering* **94** 606
[5] Jun Y W, Huh Y M, Choi J S, *et al* 2005 *Journal of the American Chemical Society* **127** 5732
[6] Gallo J, Long N J and Aboague E O 2013 *Chemical Society Reviews* **42** 7816
[7] Chen F H, Gao Q and Ni J Z 2008 *Nanotechnology* **19** 165103+9
[8] Huang H S and Hainfeld J F 2013 *International Journal of Nanomedicine* **8** 2521
[9] Panacek A, Kvitek L, Prucek R, *et al* 2006 *Journal of Physical Chemistry B* **110** 16248
[10] Jain T K, Morales M A, Sahoo S K, Leslie-Pelecky D L and Labhasetwar V 2005 *Mol Pharm* **2** 194
[11] Rosenman K D, Moss A and Kon S 1979 *Journal of Occupational and Environmental Medicine* **21** 430
[12] Kurland H D, Grabow J, Staupendahl G, Andre M E, Dutz S and Bellemann M E 2007 *Journal of Magnetism and Magnetic Materials* **311** 73
[13] Lyadov A S, Kochubeev A A, Koleva L D, Parenago O P and Khadzhiev S N 2016 *Russian Journal of Inorganic Chemistry*. **61** 1387
[14] Campos E A, Pinto D V, Sampaio de Oliveira J I, Mattos E C and Dutra L C 2015 *Journal of Aerospace Technology and Management* **7** 267
[15] Hasany S F, Abdurahman N H, Sunarti A R and Jose R 2013 *Current Nanoscience* **9** 561
[16] Hosseinian A, Rezaei H and Mahjoub A R 2011 *International Journal of Chemical and Molecular Engineering* **5** 368
[17] Teja S A and Koh P Y 2009 *Prog Cryst Growth Charact Mater* **55** 22
[18] Gupta A K and Gupta M 2005 *Biomaterials* **26** 3995
[19] Wu W, He Q and Jiang C 2008 *Nanoscale Research Letters* **3** 397